Lawrence Berkeley National Laboratory

Title

A 3-Dimensional discrete fracture network generator to examine fracture-matrix interaction using TOUGH2

Permalink

https://escholarship.org/uc/item/0n44b5w7

Authors

Ito, Kazumasa
Yongkoo, Seol

Publication Date

2003-04-09

A 3-DIMENSIONAL DISCRETE FRACTURE NETWORK GENERATOR TO EXAMINE FRACTURE-MATRIX INTERACTION USING TOUGH2

Kazumasa Ito and Yongkoo Seol

Earth Sciences Division, Lawrence Berkeley National Laboratory
One Cyclotron Road MS: 90-1116
Berkeley, CA 94720, USA
E-mail: KIto@lbl.gov

ABSTRACT

Water fluxes in unsaturated, fractured rock involve the physical processes occurring at fracture-matrix interfaces within fracture networks. Modeling these water fluxes using a discrete fracture network model is a complicated effort. Existing preprocessors for TOUGH2 are not suitable to generate grids for fracture networks with various orientations and inclinations. There are several 3-D discrete-fracture-network simulators for flow and transport, but most of them do not capture fracture-matrix interaction. We have developed a new 3-D discrete-fracture-network mesh generator, FRACMESH, to provide TOUGH2 with information about the fracture network configuration and fracture–matrix interactions. FRACMESH transforms a discrete fracture network into a 3 dimensional uniform mesh, in which fractures are considered as elements with unique rock material properties and connected to surrounding matrix elements. Using FRACMESH, individual fractures may have uniform or random aperture distributions to consider heterogeneity. Fracture element volumes and interfacial areas are calculated from fracture geometry within individual elements. By using FRACMESH and TOUGH2, fractures with various inclinations and orientations, and fracture-matrix interaction, can be incorporated. In this paper, results of flow and transport simulations in a fractured rock block utilizing FRACMESH are presented.

INTRODUCTION

Three-dimensional numerical simulation of water flow and mass transfer in fractured rock blocks is necessary to estimate the travel time of radionuclides from a radioactive waste disposal site located in unsaturated fractured rock mass. Numerical simulations of fractured rock always require careful consideration of fracture-matrix interactions, particularly in the unsaturated zone. The multiphase flow numerical simulator TOUGH2 has shown capability for modeling fracture-fracture and fracture-matrix flow. However, geometrical and physical conceptualization and mesh generation have to be done by users, and they require considerable preprocessing effort.

Several modeling programs are available for fracture-network simulations (e.g., Dershowitz et al. 1989, Billaux et al. 1989, Ijiri and Karasaki 1994). However, many of these extract fractures from fractured porous media and calculate fluid flow and/or mass transport only within fractures, neglecting fracture-matrix interactions.

The dual-continuum concept is one approach to modeling flow and mass transport in fractured porous media (Warren and Root 1963). In a dual-continuum model, fracture and matrix are modeled as two separate kinds of continua occupying the same control volume (element) in space. Fracture-matrix interaction can be modeled as the flow and transport between these continua.

To apply the dual-continuum model, we must consider the representative elementary volume (REV) and set the element volume greater than the REV. Because the maximum size of the rock block in laboratory experiments is rarely greater than one cubic meter, if fractures are few, we cannot define an REV smaller than the original block scale. In this case, the dual continuum model cannot be applied.

Another modeling approach, the discrete-fracture model, can be used with the small element volume for detailed modeling of the fractured rock mass. However, in the far field, we can neither detect all fractures in a several-kilometer area, nor make a model from all detected fractures. Thus, the discrete fracture-network model is a reasonable method to model laboratory scale fractured porous media, because at the laboratory scale, we can detect major fractures from outside surface and CT-scan observations.

For TOUGH2, a modeling method for discontinuous structures, such as a fault zone or fractured zone, was developed and applied to field tests at Yucca mountain by Doughty et al.,(2002). This model assigns new material indicators for each element including fractures. But, the interfacial areas between fracture elements and matrix elements are not considered.

With all this in mind, we developed a new mesh-generating code called FRACMESH for fractured

porous media. In this paper, we present on outline of the mesh generation and an example of numerical experiment are presented.

METHODOLOGY

Objective and Applicability of FRACMESH

FRACMESH was developed mainly for mesh preparation for simulation of flow and transport in a meter-size block. In this meter-size block, major fractures are observed on the exterior surface with various inclinations and orientations. FRACMESH generates element and connection data blocks for the TOUGH2 input file, which are the most complicated part of fracture network gridding. Preparation of other input data blocks, such as ROCKS for rock material properties and INCON for initial conditions.

Input Data for FRACMESH

To construct the TOUGH2 input data with FRACMESH, the geometrical data for the basic elements and fractures are required. The basic element data are the total length of model in x-, y-, and z- direction and the number of division in each direction. Fracture data are the number of fractures and coordinates of four corner points of each fracture and average aperture and standard deviation of each fracture.

Basic Element Construction

In FRACMESH, the basic element shape is a rectangular parallelepiped. The entire domain consists of a structured grid with constant x-, y- and z- intervals. The basic elements are automatically generated from input data, including the number of gridblocks and the interval length in each direction.

Fracture Conceptualization

In FRACMESH, each fracture is considered as a plane with a finite volume in the 3-D domain. The 3-D coordinates of the four corner points define each fracture. Each fracture has a constant or normal aperture distribution. Figure 1 shows an example of a 3-D fracture network.
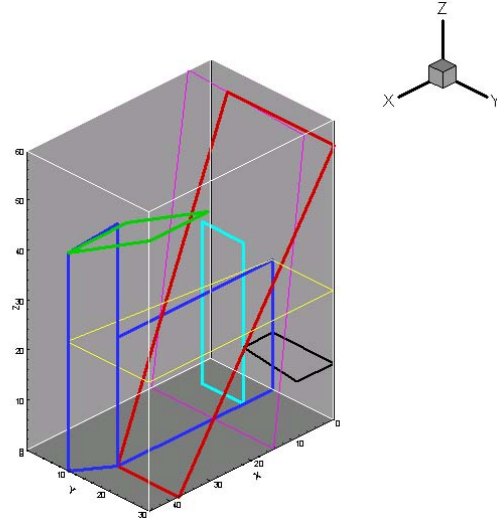

Figure 1. An example 3-D fracture model in FRACMESH.

Figure 1 is a fracture model obtained from surface observation of a 50 cm x 30 cm x 60 cm tuff block. In this model, the curve-shaped fracture illustrated in blue was represented in FRACMESH by a combination of small pieces of fracture planes with different normal vectors and corner points.

In the FRACMESH program, the factors in following equations are automatically calculated for all fractures, and the intersection of each fracture to each basic element is checked

$$ax + by + cz + d = 0, \qquad a^2 + b^2 + c^2 = 1.0 \quad (1)$$

where, (a,b,c) is the normal vector of the fracture plane.

Element and Connection Data Generation

The TOUGH2 input file requires element volume and connection information, including interfacial area and nodal distances between elements. FRACMESH automatically generates element and connection data from fracture information in the model, based on the fracture-network configuration and predefined elemental information (grid number and interval length).

Classification of basic elements

All elements are classified into one of two groups, matrix elements or fracture elements. If at least one of the finite fracture planes crosses a basic element, that element is considered a fracture element. Otherwise, it is considered a matrix element.

In FRACMESH, classification is made in two steps. The first step is the judgment on whether each edge of an element and each fracture intersect when the

fracture is assumed to be infinite (See Figure 2). If an edge of an element is judged to cross a fracture, the x, y, and z coordinates of the crossing point are calculated from the equation of the fracture plane. In the second step, the crossing point is judged to be in the finite fracture plane or not by comparing the summed area of four triangles (formed by the crossing point and two adjacent corner points of fracture) to the area of finite fractures.
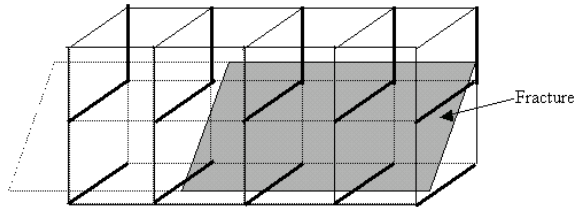

Figure 2. Grouping of element edge by the intersection of an infinite fracture. The hatched area is the finite fracture plane, and thick lines are the edges that intersect the infinite fracture plane.

Element volume

The element volume of the matrix element is set equal to the basic element volume. An element volume of a fracture element is calculated as the total volume of fractures inside the element.

Connection configuration

The element-by-element connections are classified into three types: i.e. fracture-fracture, fracture-matrix, and matrix-matrix connections. At first, the basic connection is set to be the structural connection between adjacent elements in 3-D the grid. After the generation of fracture elements, connections between two elements, which are directly connected by at least one fracture, are classified as fracture-fracture connections. If neither element contains any fractures, the connection between these two elements is set as matrix-matrix type. If either element contains fractures but the fractures do not directly connect both elements, the connection between these two adjacent elements is set as fracture-matrix type.

A schematic diagram illustrating connection type is shown in Figure 3.
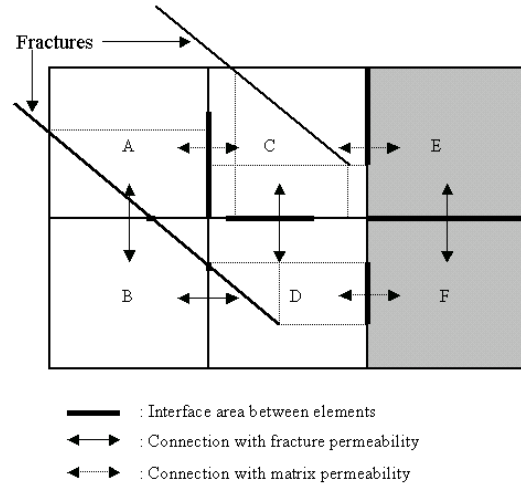

Figure 3. Schematic diagram of connection configuration for adjacent elements. Shaded elements are matrix elements. Solid arrows show the fracture-fracture connection, and dotted arrows show the matrix-fracture and matrix-matrix connection.

In Figure 3, connections between A-B and B-D are the fracture-fracture connections, E-F is the matrix-matrix connection, and A-C, C-D, C-E, and D-F are the fracture-matrix connection. TOUGH2 input data requires the nodal distance in both adjacent elements and interfacial area in the connection data block. In FRACMESH, nodal distance is assumed to be the distance between the center of the basic gridblock and the interface between the two gridblocks.

Interfacial area is determined as follows. In matrix-matrix connections, the interfacial area is the same as the interfacial area between basic gridblocks. In the fracture-fracture connections, interface area is calculated differently, depending on the option chosen for the aperture distribution. (Aperture distribution can be uniform or random.) The interfacial area is assumed to be the aperture of fractures that cross the interface. If the random permeability distribution option is chosen, the aperture at the interface is assumed to be the average of the two aperture values in adjacent elements.

The fracture-matrix connection is the most important connection for flow and transport between fracture and matrix. In FRACMESH, the interfacial area is defined from a projected area of the fracture to the interface. If one of the two adjacent elements contains one fracture, the interfacial area is the projected area of the fracture to the interface (see connection C-E in Figure 3). If both elements contain fractures; the interfacial area is the average of the two projections (see connection A-C, C-D in Figure 3). If

either element contains multiple fractures, the projected areas are averaged.

In FRACMESH, nodal distances in gridblocks are assumed to be half of the grid length in each direction.

Dummy element generation for boundary conditions

In FRACMESH, side boundaries are automatically set as no-flow boundaries. FRACMESH adds top and bottom dummy elements, with top elements acting as either a constant head boundary, or a constant flow rate boundary. Bottom elements can be a constant head boundary or a free drainage boundary (TOUGH2 implementation in iTOUGH2 only). All connections between boundary elements and elements in the main area are automatically generated with zero nodal distance.

Permeability Distribution of Fracture Elements

In TOUGH2, element-by-element permeability distributions can be realized using a permeability modification factor. In a single fracture, FRACMESH utilizes the permeability distribution factor to provide heterogeneity in the aperture distribution. For input data, users set the average hydraulic apertures and standard deviations in individual fractures. Based on the normal distribution model, the local aperture in a fracture segment within an element is calculated.

To alter the aperture, we assign each fracture segment a permeability modification factor determined by fracture surface roughness observations (Mongano et al., 1999). Permeability and capillary pressure for each fracture are modified as follows (Leverett, 1941; Pruess et al., 1999):

$$k_f = k_{ave} \cdot m \qquad (2)$$

$$P_c = \frac{P_{c,ave}}{\sqrt{m}} \qquad (3)$$

In these relations, k_f is the permeability of a fracture segment, k_{ave} is the average permeability of a fracture calculated by the cubic law, m is the permeability modification factor, P_c is the capillary pressure of a fracture segment, and $P_{c,ave}$ is the average capillary pressure of a fracture. Using the permeability modification factor, heterogeneity in aperture, permeability, and capillary pressure can be incorporated for individual fractures as well as for each element in a fracture.

AN EXAMPLE OF DISCRETE FRACTURE MODEL AND SIMULATION

Model Construction

Vertical 2-D simulations of water flow and tracer transport were carried out as a preliminary study for meter-size block experiments (Seol et al., 2003). A fracture network was artificially generated based on statistical information derived from detailed line survey observations including fracture density, length range, and distribution of directions for a tuff unit, called lower lithophysal unit in Yucca Mountain. Fractures with different trace lengths and orientations obtained from field observations were sorted into groups and counted to calculate the occurrence probability of fractures for each fracture group. For our artificial fracture-network generation, a fracture was located at random and independently assigned a trace length and orientation based on the occurrence probability. The total number of fractures to be generated was determined using the fracture line density (the number of fractures per unit length in the horizontal or vertical direction). The fracture density for the lower lithophysal unit was 3.2 fractures/m (Liu et al., 2000). However, the density was doubled to 6.4 fractures/m, because the fracture network needed to account for the limited connectivity of fractures in the 2-D flow domain to address a 3-D flow regime. Doubling the fracture density provided a model block with several flow pathways in a small scale flow field (1.0 m × 1.0 m). To assure that the developed model block was consistent with the overall distribution of fractures under natural conditions, we generated a larger-scale fracture network (10 m × 10 m) based on the same statistical information, and then the 1.0 m x 1.0 m fracture network was visually compared to the 10 m x 10 m network. In general, the fracture network for the study shows reasonable resemblance to many areas from the larger network.

In addition to the simulated fracture network capturing large fractures based on the detailed line survey, we also added small fractures using small fracture survey data (CRWMS M&O, 1999). We did this to compensate for small fractures (<1.0 m) ignored in the detailed line survey. Large fractures control global flow through the fracture system, whereas small fractures significantly impact interfacial phenomena between fracture and matrix by providing more interface area to the system (Wu et al., 2003).
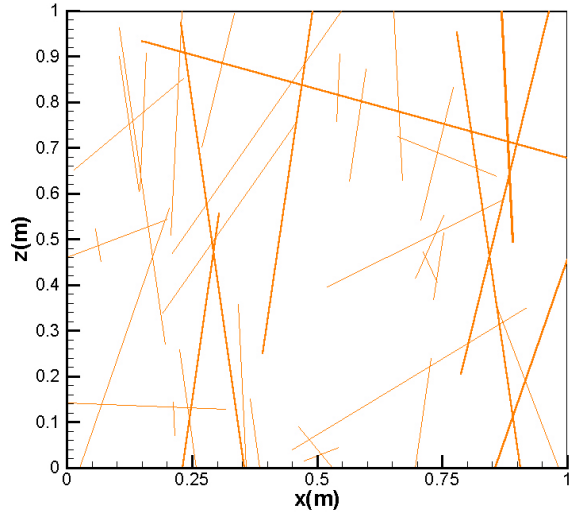
Figure 4. Discrete fracture network model constructed from stochastic data obtained from field survey.

The 2-D model (1.0 m × 1.0 m, with a thickness of 0.01 m) contains 39 fractures of various lengths and orientations (Figure 4). The aperture is correlated to fracture length as described by Liu et al., 2001. Based on the relationship between fracture trace length and filling material (Chiles and de Marsily, 1993), the average aperture, *b*, is calculated using an empirical equation with trace length, *L* (m):

$$b = cL^d \qquad (4)$$

where *c* and *d* are empirical constants determined to be 1.008×10^{-5} and 0.317, respectively, for representative mean and variance values of log(*b*) for the TSw in Yucca mountain NV. (–4.01 and 0.05, respectively) (Liu at al., 2000; Robinson, 2000). For the TOUGH2/iTOUGH2 code (Pruess et al, 1999; Finsterle, 1999), the fracture network was transformed into a mesh with 3,750 grid elements. Both matrix and fracture elements had uniform dimensions [0.0133 m × 0.02 m × 0.01 m (L×W×T)]. Matrix elements had a uniform volume, whereas the volume in a fracture element was calculated using the fracture aperture and trace length of the fracture segment cross-cutting the element. Table 1 shows hydraulic parameters of fracture and matrix elements used in this simulation.

We carried out transient unsaturated water flow simulations and pseudo steady-state tracer transport simulations. Water was injected at various rates until the outflow rates reached 99% of inflow rates. The balanced state is defined herein as pseudo-steady state, which indicates that the flow system did not reach a true steady state, but overall flow rates are balanced. Once a balance in flow rates was achieved, a given mass of tracer was placed into the model blocks through one large injection element on top of each block. The mass of tracer exiting the block was monitored to plot the breakthrough curves.

Table 1. Input parameters for TOUGH2/iTOUGH2

	Fracture	Matrix
Density (g/cm^3)	2.48	2.48
Porosity	1.00	0.131
Absolute permeability (m^2)	4.51E-11	3.04E-17
Tortuosity	0.7	0.7
Residual liquid saturation	0.01	0.12
Residual gas saturation	0.01	0.02
Initial liquid saturation	0.02	0.55
m, 1-1/n $_*$	0.611	0.236
α	7.39E-4	6.44E-6

* Corey's curve (Corey, 1954) is used for relative permeability, and the modified van Genuchten model (van Genuchten, 1980, Finsterle, 1997) is used for capillary pressure.

Results and Discussion

Transient State Unsaturated Flow Experiments

The model blocks were initially saturated as high as 45% liquid saturation in matrix and 1% in fractures. At this low matrix saturation, most of tracer injected would quickly imbibe from fractures to matrix, and a breakthrough for a tracer pulse would not take place during a reasonable time frame for laboratory experiments. As a consequence, transient experiments were designed to monitor only water flow rates at the bottom of the block with various injection rates.

The injection rate was set as various ratios of the saturated steady state flow rate. Table 2 shows the injection rate and corresponding infiltration rate.

Table 2. Injection rates

[a]Flow Rate (%)	Flow Rate (kg/s)	Injection Rate (ml/day)	Infiltration (mm/year)
0.02	7.12E-09	0.6	22.5
0.1	3.56E-08	3.08	112.27
0.2	7.12E-08	6.2	224.5
1	3.56E-07	30.8	1122.7
2	7.12E-07	61.5	2245.4
10	3.56E-06	307.6	11226.8
20	7.12E-06	615.0	22454.0

[a] Flow rate as a percentage(%) of maximum flow rate measured from fully saturated block test
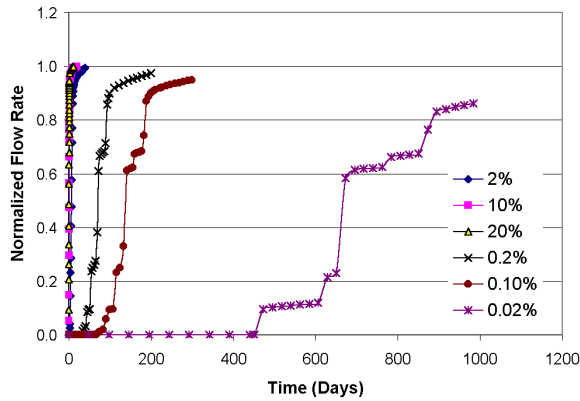

Figure 5. Water breakthrough curves in DFNM with various injection flow rate as a percentage of saturated flow rate

Figure 5 shows normalized flow rates, which increase as a function of time and approach to steady state. Stepwise increases of outflow with low injection rates (<2% of maximum flow rate) represents localized preferential flow predominantly through fractures. At higher flow rates, water flows fast enough to reach the bottom of the block through limited preferential flow pathways (such as fractures) and quickly attains the balanced state in terms of flow rates (even though a significant portion of the matrix block is still dry). Therefore, it is difficult to observe discrete flow behavior unless very fine observation frequency is utilized.

Liquid saturation distributions as a function of time and injection rates show flow channelling (preferential flow pathways) as a higher liquid saturation for higher injection rate cases (Figure 6).

The discrete behavior of liquid saturation would result from variations in fracture aperture size and heterogeneity implemented by the permeability modification factor. Liquid saturation distributions are quite distinctive for different injection rates. Most of the water introduced at lower injection rates diffuses into the matrix. Then, when the water reaches the bottom, a large portion of the matrix on the pathway of water flow is nearly saturated. Water flow is predominantly governed by capillary pressure at low injection rates. On the other hand, higher injection rates result in gravity-driven water flow mainly through fractures, so that high liquid saturation is limited to the area near fractures when water reaches the bottom of the block.
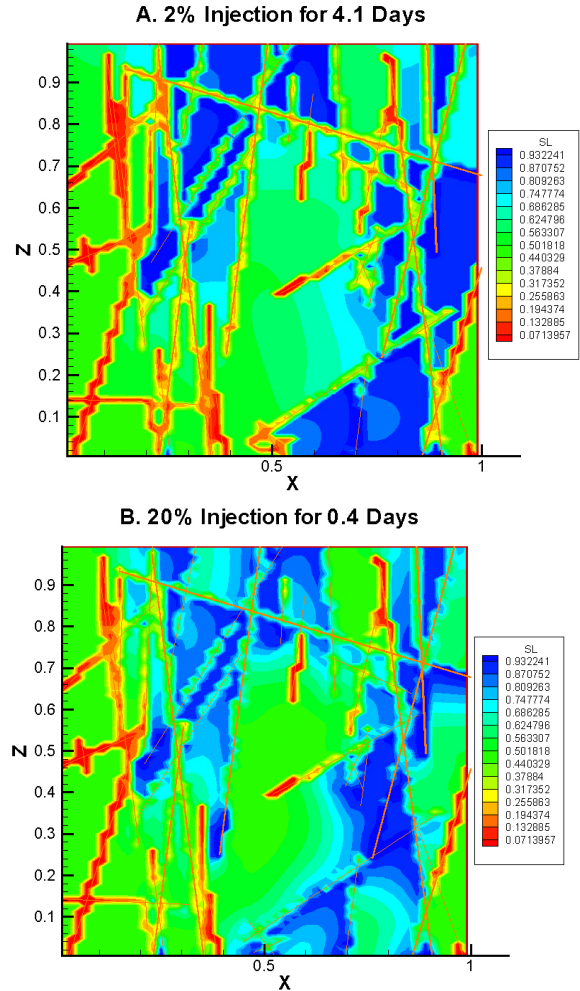

Figure 6. Distribution of water saturation in discrete fracture network model with different injection flow rates

Pseudo-steady unsaturated flow and transport experiments

Various water-injection rates were also applied to the unsaturated (45% in matrix, 1% in fracture) block. Once the balance between injection rates and effluent flow rates was achieved, the same mass of tracer in a same volume of water was injected into the block and then monitored to plot breakthrough curves. The median front of the tracer breakthrough curves arrived at the bottom of the block at 0.3, 0.1, and 0.08 days, for injection rates of 2%, 10%, and 20% of saturated flow rates, respectively (Figure 7).
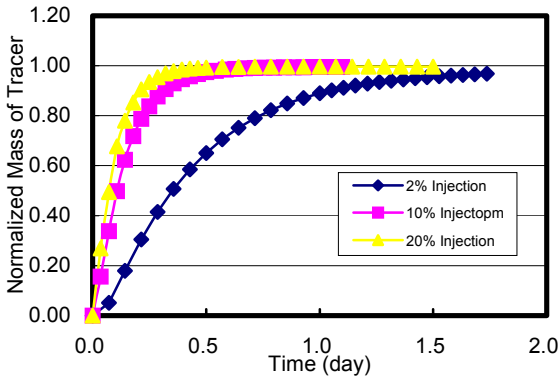
Figure 7. Tracer breakthrough curves. For various injection rate at balanced condition.

Under pseudo-steady-state conditions, the tracer breakthrough curves do not show the stepwise increase even at small injection rates, because the capillary pressure values of fracture and matrix elements are in equilibrium.

SUMMARY

In this study, a new mesh generator for fractured porous media, FRACMESH, was developed and applied to vertical 2-D unsaturated water flow and tracer transport modeling with TOUGH2.

In unsaturated water flow simulations, preferential water pathways caused by fractures and water flow from fractures to matrix caused by capillarity could be simulated by TOUGH2 with FRACMESH. For small injection rates, stepwise water breakthrough was observed because of the multiple dominant water pathways. In tracer-transport simulations under pseudo-steady-state conditions, tracer pathways were limited to fractures, and the injection rate controlled the tracer breakthrough curve. From these simulations, TOUGH2 with FRACMESH has proved capable of modeling the flow and fracture-matrix interactions in fractured porous media when dominant fractures can be observed. We are planning to apply FRACMESH to an actual 3-D meter-size block for the design of actual laboratory experiments.In addition, comparison studies between FRACMESH-TOUGH2 simulations and other discrete-fracture-network model simulations will be performed for more strict validation of the code.

ACKNOWLEDGMENTS

REFERENCES

Billaux, D., K. Karasaki, and J. Long, A Numerical Model for 3-Dimensional Modeling of Channelized Flow in Rocks, *Proceedings, International Association of Hydrology Conference, Paris*.1989.

Chiles, J.-P., and D. de Marsily, Stochastic modeling of fracture systems and their user in flow and transport modeling. In Bear, J. Tsang, C.F., de Marsily D. (Eds). *Flow and Contaminant Transport in Fractured Rock,* pp. 169-231. Academic Press. San Diego, CA. 1993.

Corey, A. T. The interrelation between gas and oil relative permeabilities, Producers Monthly, 38-41, November 1954

CRWMS M&O, Detailed Line Survey Data for Horizontal and Vertical Traverses, ECRB TDIF: 308976. CRWMS M&, Las Vegas, NV. 1999.

Dershowitz, W., A. Herbert, and J. Long, *Fracture Flow Code Cross Verification Plan*, SKB Stripa Project Technical Report TR 89-02, SKB, Stockholm, Sweden,1989

Doughty,C., R. Salve, and J.S.Y. Wang, Liquid-release tests in unsaturated fractured welded tuffs: II. Numerical modeling*, J. Hydrol*., 256, 80-105, 2002

Finsterle, *iTOUGH2 Command Reference*, Report LBNL-40041, Lawrence Berkeley National Laboratory, Berkeley, Calif. 1999

Ijiri, Y., and K. Karasaki, A Lagrangian-Eularian Finite Element Method with Adaptive Gridding for Advection-Dispersion Problems, *X International Conference on Computational Methods in Water Resources*, Heidelberg, Germany, July pp.19-22.

Leverett, M.C., Capillary behaviour in porous media, *Tran. Soc. Pet. Eng. AIME*, 142, 152-269, 1941.

Liu H.H., D.F. Ahlers, M.A. Cushey, *Analysis of Hydrologic Properties Data,* ANL-NBS-HS-000002 REV 00, Analysis Modeling Report, Yucca Montain Nuclear Waste Disposal Project, Lawrence Berkeley National Laboratory, Berkeley, CA., CRWNS M&O, Las Vegas NV.

Mongano G.S., W.L. Singleton, T.C. Moyer, S.C.Bearson, G.L.W. Eatman, A.L. Albin, and R.C.Lung, *Geology of the ECRB cross drift – Exploratory Studies Facility, Yucca Mountain Project, Yucca Mountain, Nevada,* Bureau of Reclamation and U.S. Geological Survey, Denver, Colorado, 1999.

Pruess, K., C. Oldenburg, and G. Moridis, *TOUGH2 User's Guide, Version 2.0*, Report LBNL-43134,

Lawrence Berkeley National Laboratory, Berkeley, Calif., 1999. :

Seol, Y., T. Kneafsey, K. Ito, and S. Finsterle, Two-D Simulations of Flow and Transport on a Meter-Sized Unsaturated Fractured Tuff Block, In Preparation.

van Genuchten, M. A Closed-Form Equation for Predicting the Hydraulic Conductivity of Unsaturated Soils. *Soil Sci. Soc. Am. J., 44,* 5, 892–898, 1980

Wu, Y.-S., H.H.Liu, and G.S. Bodvarsson, A triple-continuum for flow and transport processes in fractured rocks. submitted *to J. Contam. Hydrol.,* 2003